Inorganic Chemistry

Communication

pubs.acs.org/IC

Crystal Structure and Electronic Properties of Y_3AlC_3

Martin R. Kotyrba,[†] Eduardo Cuervo-Reyes,[‡] and Reinhard Nesper*,[†]

[†]Laboratory of Inorganic Chemistry, ETH Zurich, Vladimir-Prelog Weg 1−5/10, 8093 Zurich, Switzerland

[‡]Reliability Science and Technology, EMPA Dübendorf, Überlandstrasse 129, 8600 Dübendorf, Switzerland

Supporting Information

ABSTRACT: A novel ternary aluminum carbide, Y_3AlC_3, has been synthesized under application of a lithium metal flux at high temperature (1523 K). Single-crystal structure determination of this compound revealed a new structure type with the Wyckoff sequence 2j3e and remarkable structural features at the border between Zintl and intermetallic phases. The puzzling bonding structure of Y_3AlC_3 is analyzed with the aid of electronic structure calculations (energy bands and the electron localization function).

Most ternary transition-metal aluminum carbides can be classified into three different structural settings, i.e., based on the Perovskite type, the $ScAl_3C_3$ structure (alternating layers of binary carbides), and layered systems between carbide substructures and interlaced metal.[1−5] Few exceptions from these are known, some of which show surprising bonding features like $Th_2Al_2C_3$[6] or YAlC,[7] having either f- or d-orbital-mediated Al−Al bonding. The occurrence of such compounds indicates that ternary transition-metal aluminum carbides have a larger and significantly more complex structural diversity than originally thought.

Here we report the new phase Y_3AlC_3 [space group *Pmma* (No. 51)] with a singular structure type (Wyckoff sequence 2j3e) in the Y−Al−C system. In reference to our report in 7, Y_3AlC_3 constitutes another example of an intermetallic compound, where (interestingly) the electron count can be forced to fit a closed-shell model.

At the first glance, a carbide of composition $M^{III}_4C_3$ would be thought of as a classical methanide like, for example, Al_4C_3. The structural features of Y_3AlC_3 though indicate much more complex chemical bonding, raising the question of why simple valence rules do not apply here. The crystal structure is shown (Figure 1, left) as an octahedral network next to a projection of the unit cell along the *b* axis (Figure 1, right).

The network is set up by four different, distorted octahedral surroundings formed by Y and Al atoms, two of which contain either a central C atom or a C_2 dumbbell (cf. *A* and *B* in Figure 1), while the others are void (*C* and *D* in Figure 1). Endohedral carbon dumbbells are located within Y_6 octahedra (Figure 1, *A*) pointing to not fully reduced anionic carbon moieties. The dumbbell length $d(C_I{-}C_I) = 1.308(1)$ Å is comparable to $d(C{-}C) = 1.298$ Å in YC_2,[8] corresponding to a double-bonded ethenide unit. The distances from C_I to the $Y_I/Y_{II}/Y_{IV}$ positions are $d(C_I{-}Y_I) = 2.680(1)$ Å, $d(C_I{-}Y_{II}) = 2.349(1)$ Å, and $d(C_I{-}Y_{IV}) = 2.557(1)$ Å and compare well with the distances found, for example, in YC_2[8] and Y_4C_5.[9] The edges of the octahedron are between 3.564(1) and 4.255(1) Å in length. The largest value is unusually long, which may arise from the nonspherical anion in the center, and lies between the radii of the first and second coordination spheres found in most of the binary yttrium carbides. The center of mass (O_I) of the dumbbell is at (*x*, 0.5, *z*), having site symmetry 0.2/*m* [the distorted Y_6 octahedron has C_{2h} symmetry, with angles $\angle Y_IY_{II}Y_{III} = 49.52(1)°$, $\angle Y_{II}Y_IY_{II} = 65.24(2)°$, $\angle Y_IO_IY_{II} = 100.18(1)°$, and $\angle Y_{II}O_IY_{IV} = 79.81(1)°$]. The isolated methanide center C_2 is also surrounded by a

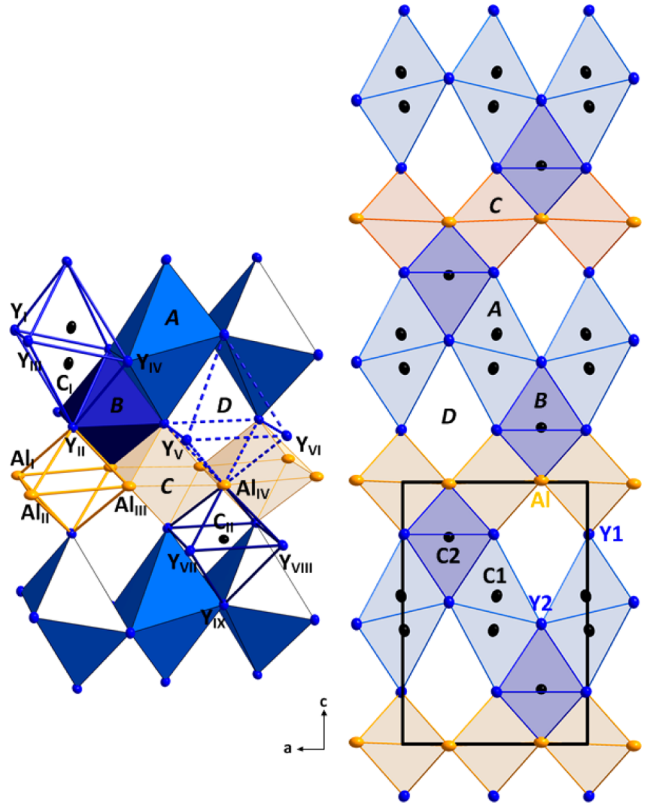

Figure 1. Crystal structure of Y_3AlC_3 represented as a polyhedral network. The different octahedra are denoted by italic letters. The atoms at the corners are named using different roman subindices (despite symmetry equivalences) in order to facilitate the description of distances and angles. The rectangular frame (right) displays the projection of the elementary cell.

Special Issue: To Honor the Memory of Prof. John D. Corbett

Received: October 1, 2014
Published: November 25, 2014

   dx.doi.org/10.1021/ic5023664 | *Inorg. Chem.* 2015, 54, 710−712

distorted octahedral environment Y_5Al, in this case having C_{2v} symmetry. $d(Al_{IV}-C_{II})$ is of length similar to that in Al_4C_3 despite the higher coordination number of carbon, i.e., 6 vs 4. Y_{II} is the apex of Y_2Al_4 surrounding of the octahedral void C (Figure 1) with the center-of-mass O_{II} and C_{2h} point symmetry. The mutual edge sharing of these Y_2Al_4 octahedra sets up a nearly quadratic aluminum grid with $d(Al_I-Al_{II})$ = 3.654(1) Å and $d(Al_I-Al_{II})$ = 3.515(1) Å, which has a weak wavelike modulation along the a axis. The Y−Al distances are $d(Y_{II}-Al_I)$ = 3.265 Å and $d(Y_{II}-Al_{III})$ = 3.119 Å. The angles $\angle Al_IY_{II}Al_{II}$ = 66.16(1)°, $\angle Al_{II}Al_IY_{II}$ = 56.92(1)°, $\angle Al_IO_{II}Y_{II}$ = 92.70(1)°, and $\angle Y_{II}O_{II}Al_{III}$ = 87.30(1)° mark the distortion.

The void D has a distorted octahedral Y_5Al coordination with C_{2v} symmetry (Figure 1, D). Equivalent D voids are stacked along the b axis, sharing the Y_V-Y_{VI} edge. This arrangement results in one-dimensional channels along the b axis.

Y_3AlC_3 is best described as a blend of an intermetallic with a Zintl phase. As shown in Figure 2, there are two half-filled bands (per formula unit), both of which have significant contributions of Al p and Y d orbitals.

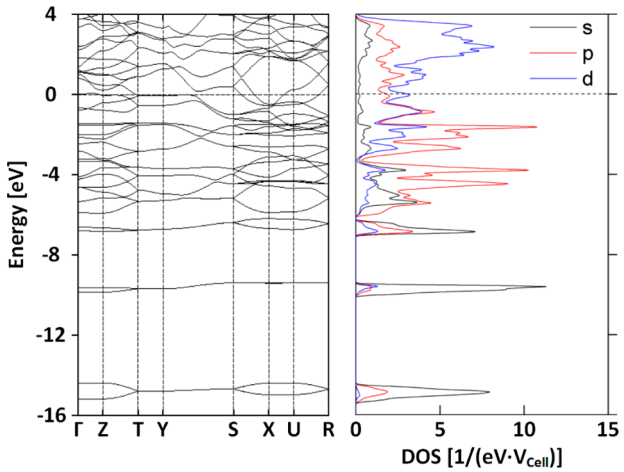

Figure 2. Band structure (left) and partial density of states (right) of Y_3AlC_3.

The most reasonable simplified charge partitioning is $[Y^{3+}]_3[Al^+][C^{4-}][C_2]^{4-}(e^-_2)$. The two extra electrons correspond to the incompletely filled bands, whose role in the bonding will become clear later. The primitive cell contains two formula units (f.u.); therefore, Figure 2 shows two bands per orbital type in the f.u., which are degenerate along the segments T−Y and Y−S in reciprocal space. First and third doublets correspond to bonding and antibonding combinations of the C1 s states. The second doublet originates mainly from C2 s. The Al s orbital, despite being slightly more spread in energy, mainly contributes to the fourth band and is fully below the Fermi level (E_F). All C2 p orbitals are found mainly below E_F, supporting our interpretation of it as a methanide with no covalent bonding to aluminum. This can be also derived from the electron localization function (ELF; Figure 3).

There is no ELF attractor between aluminum and carbon. Al p orbitals are high in energy and mostly mix with (are stabilized by) the Y d states, contributing to the conduction bands. This lack of Al−C covalency should not be interpreted as a fully ionic interaction; we prefer to see it as having C^{4-} anions embedded in a metallic sea. In fact, the ELF shows little variation over an extended and fully connected region (the aluminum plane). This

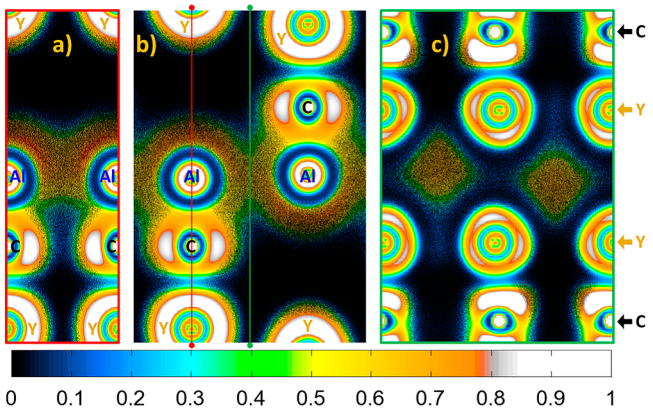

Figure 3. Planar cuts of the ELF and electron density. The red and green lines in part b indicate where the perpendicular cuts (a and c) were taken, respectively.

is a modulated plane net (Figure 3a−c), where the long distance between the aluminum centers is bridged by Y d orbitals. Such a "homogeneous" distribution suggests a metallic-like bonding interaction involving aluminum and yttrium, which contributes to the bands across the Fermi level. The high localization toroid around C_2, perpendicular to the Al−C−Y axis (Figure 3a,b), results from the two C p states that are orthogonal to the Al s orbital and thus also indicates lone electron character on the carbon.

The carbon dumbbell has a shorter bonding length than C_2^{4-} in other ethenid compounds[10,11] and is similar to the one in YC_2[8], where the antibonding C p orbitals are part of the conduction band. The site-resolved partial density of states (Figure 4) reveal that this is also the case for Y_3AlC_3 with a weak

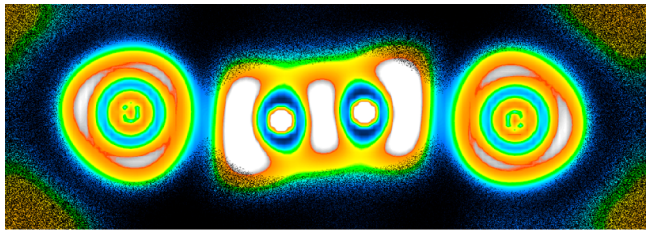

Figure 4. C_2^{4-} dumbbell with two yttrium corners of the surrounding Y_6 octahedra (left and right of the dumbbell).

contribution of the corresponding states around E_F. The tilted stacking of the dumbbell along the b axis suggests that the direct overlap of the C1 orbitals of different dumbbells is not significant and their weak contribution to a conduction band is indirect, through a mixing of the antibonding C1 p orbitals with the Y d orbitals. As such, a tiny part of the C_2^{4-} anion-based charge is given back to the Y d states, which results in a slight increase in the effective bond order and a shortening of the dumbbell. The ELF of the C_2 anion is strongly distorted (Figure 2), as expected because of mixing with the yttrium orbitals. In a similar fashion, the partial occupation of the antibonding states, and their mixing with Y d orbitals, results in a distortion of the cation sphere. Note the significant differences between the ELFs of the two nonequivalent yttrium sites. Y2 cations, being around the waist of the dumbbells and not being affected by antibonding states, have rather spherical shells. Y1 cations, which interact with aluminum and face the antibonding states of the dumbbells, show significant distortion. In accordance with this, the Mulliken

dx.doi.org/10.1021/ic5023664 | Inorg. Chem. 2015, 54, 710−712

population analysis projects on Y1 a larger amount of the electron density than on Y2.

Interestingly, the electron count also fits closed-shell model $[Y]_3^{3+}[AlC]^{5-}[C_2]^{4-}$ with an overcharged AlC unit. The actual electron distribution may be seen as a relaxed version of this limiting valence model. From the formal number of electrons, the $[AlC]^{5-}$ anion is to be considered as an ethenide analogue with aluminum substitution. It is obvious that the high negative charge (higher than that in C_2^{4-} because of aluminum substitution) is less realistic. Actually, not only the Al p states but also the antibonding combination of Al s and C p_z mix with Y d orbitals in the conduction band.

It is not yet clear why the new intermetallic ternary carbide Y_3AlC_3 exists in this "closed-shell alike" stoichiometry. Nevertheless, we do have evidence in other compounds in the Y−Al−C family, where "magic" numbers are also combined with unusual structures.[7,12] As in many intermetallics, valence rules and the Zintl−Klemm concept cannot be utilized for prediction of the structure but a shadow of the valence concept remains visible, at least. Clearly, with such compounds, an interesting gray zone opens at the border between the Zintl and intermetallic phases, which makes the set of chemical bonding patterns even richer.

ELF values are shown by the color of the pixels, according to the scale defined at the bottom of Figure 3. The fraction of colored pixels (over a black background) is proportional to the electron density (ρ), relative to a reference value of $\rho_0 = 5 \times 10^{-3}$ $e^-/Å^3$ (the typical value for poor metals). This means that at any given point the pixel is left black with probability $p = 1 - \min(1, \rho/\rho_0)$. The use of a saturation value (ρ_0) in the density scale is necessary in order to soften the dazzling higher densities at the cores, which have no chemical interest and would otherwise hide the softer features related to chemical bonding. The figures were made using a plotting code developed in house, which makes use of the data obtained within linear muffin-tin orbital (LMTO) calculations.

The electronic structure was calculated using several implementations of the density functional theory (DFT) approach. We employed the *CASTEP* and *Dmol3* packages within *Materials Studio* and the LMTO-atomic sphere approximation (ASA) code from Stuttgart. This allowed us to check that the relevant results were independent of the type of orbital basis and treatment of the interaction within the DFT approach. Plots of energy-resolved states (bands and density of states) were taken from *Dmol3* calculations with the POB functional. The data for real-space plots (electron density and ELF) were taken from LMTO-ASA calculations. Details on the calculation settings can be provided if necessary.

■ ASSOCIATED CONTENT

Supporting Information

X-ray crystallographic data in CIF format, synthetic details, and information on structure determination and powder diffraction for Y_3AlC_3. This material is available free of charge via the Internet at http://pubs.acs.org.

■ AUTHOR INFORMATION

Corresponding Author

*E-mail: nesper@inorg.chem.ethz.ch. Fax: (+41) 44 632 1149.

Author Contributions

The manuscript was written through contributions of all authors. All authors have given approval to the final version of the manuscript.

Notes

The authors declare no competing financial interest.

■ ACKNOWLEDGMENTS

We are thankful to B. Battlog and J. Kanter for kindly measuring the electronic conductivity on single crystals. This work was funded through the Swiss National Science Foundation under Grant 2000-20132788.

■ DEDICATION

In memory of Professor John. D. Corbett.

■ REFERENCES

(1) Rosen, S.; Sprang, P. G. *Adv. X-Ray Anal.* **1965**, *8*, 91−102.
(2) Tsokol, A. O.; Bodak, O. I.; Marusin, E. P.; Baivel'man, M. G. *Kristallografiya* **1986**, *31*, 791−792.
(3) Schuster, J. C.; Nowotny, H.; Vaccaro, C. *J. Solid State Chem.* **1980**, *32*, 213−219.
(4) Jeitschko, W.; Nowotny, H. *Monatsh. Chem.* **1967**, *98*, 329−337.
(5) Hu, C.; Li, F.; Zhang, J.; Wang, J.; Wang, J.; Zhou, Y. *Scr. Mater.* **2007**, *57*, 893−896.
(6) Gesing, T. M.; Jeitschko, W. *J. Alloys Compd.* **1996**, *240*, 9−15.
(7) Kotyrba, M.; Cuervo-Reyes, E.; Nesper, R., in preparation.
(8) Yosida, Y. *J. Appl. Phys.* **2002**, *92*, 5494−5497.
(9) Czekalla, R.; Hufken, T.; Jeitschko, W.; Hoffmann, R.-D.; Pottgen, R. *J. Solid State Chem.* **1997**, *132*, 294−299.
(10) Mattausch, H.; Kienle, L.; Duppel, V.; Hoch, C.; Simon, A. *Z. Anorg. Allg. Chem.* **2009**, *635*, 1527−1535.
(11) Carrillo-Cabrera, W.; Curda, J.; Peters, K.; Kohout, M.; von Schnering, H. G. *Z. Anorg. Allg. Chem.* **2004**, *630*, 2186−2190.
(12) Kotyrba, M.; Cuervo-Reyes, E.; Nesper, R., in preparation.